Projected increases in the annual flood pulse of the Western Amazon

2016 Environ. Res. Lett. 11 014013

(http://iopscience.iop.org/1748-9326/11/1/014013)

Environmental Research Letters

LETTER

Projected increases in the annual flood pulse of the Western Amazon

Zed Zulkafli[1,2], Wouter Buytaert[1,3], Bastian Manz[1], Claudia Véliz Rosas[4,5], Patrick Willems[6], Waldo Lavado-Casimiro[7], Jean-Loup Guyot[8] and William Santini[8,9]

[1] Department of Civil and Environmental Engineering, Imperial College London, London, UK
[2] Department of Civil Engineering, Universiti Putra Malaysia, Serdang, Malaysia
[3] Grantham Institute for Climate Change and the Environment, Imperial College London, London, UK
[4] Centro de Datos para La Conservación, Universidad Nacional Agraria La Molina, Lima, Peru
[5] World Wildlife Fund (WWF), Lima, Peru
[6] Hydraulics Laboratory, Katholieke Universiteit Leuven, Belgium
[7] Servicio Nacional de Meteorología e Hidrología (SENAMHI), Lima, Peru
[8] Institut de recherche pour le développement (IRD), Lima, Peru
[9] Géosciences Environnement Toulouse (GET), Lima, Peru

E-mail: z.zulkafli10@imperial.ac.uk

Keywords: Peruvian Amazon, hydrological extremes, climate change impact

OPEN ACCESS

RECEIVED
28 July 2015

REVISED
15 December 2015

ACCEPTED FOR PUBLICATION
17 December 2015

PUBLISHED
27 January 2016

Abstract

The impact of a changing climate on the Amazon basin is a subject of intensive research because of its rich biodiversity and the significant role of rainforests in carbon cycling. Climate change has also a direct hydrological impact, and increasing efforts have focused on understanding the hydrological dynamics at continental and subregional scales, such as the Western Amazon. New projections from the Coupled Model Inter-comparison Project Phase 5 ensemble indicate consistent climatic warming and increasing seasonality of precipitation in the Peruvian Amazon basin. Here we use a distributed land surface model to quantify the potential impact of this change in the climate on the hydrological regime of the upper Amazon river. Using extreme value analysis, historical and future projections of the annual minimum, mean, and maximum river flows are produced for a range of return periods between 1 and 100 yr. We show that the RCP 4.5 and 8.5 scenarios of climate change project an increased severity of the wet season flood pulse (7.5% and 12% increases respectively for the 100 yr return floods). These findings agree with previously projected increases in high extremes under the Special Report on Emissions Scenarios climate projections, and are important to highlight due to the potential consequences on reproductive processes of in-stream species, swamp forest ecology, and socio-economy in the floodplain, amidst a growing literature that more strongly emphasises future droughts and their impact on the viability of the rainforest system over greater Amazonia.

1. Introduction

As one of the world's largest biodiversity hotspots and carbon stocks, the vulnerability of the Amazon basin to changing climate conditions is a subject of intensive research [1, 2]. A major direct impact of climate change is the risk of forest dieback (savannisation) because of climatic drying in the lower Amazon [3–6]. Climate change will also affect the hydrological regulation (flood buffering capacity) and extremes, and there have been growing efforts to understand such dynamics at sub-regional scales such as in the Western upper branches of the Amazon [2, 7, 8].

Emerging evidence suggests that changing climate conditions in the Western Amazon are affecting the flood buffering capacity of the basin and consequently the ecological and socio-economic processes that it supports [2]. In 2010, a prolonged period of low flows disrupted river transport and triggered an outburst of water-borne diseases. This event was followed by a rapid change from hydrological drought conditions to historical high flows in 2012, which caused high sediment yield and transport in the river. Yet, long-term historical evidence of climate change and its impact on the local water cycle is scarce and based on a relatively short period of records. Annual maximum flows show

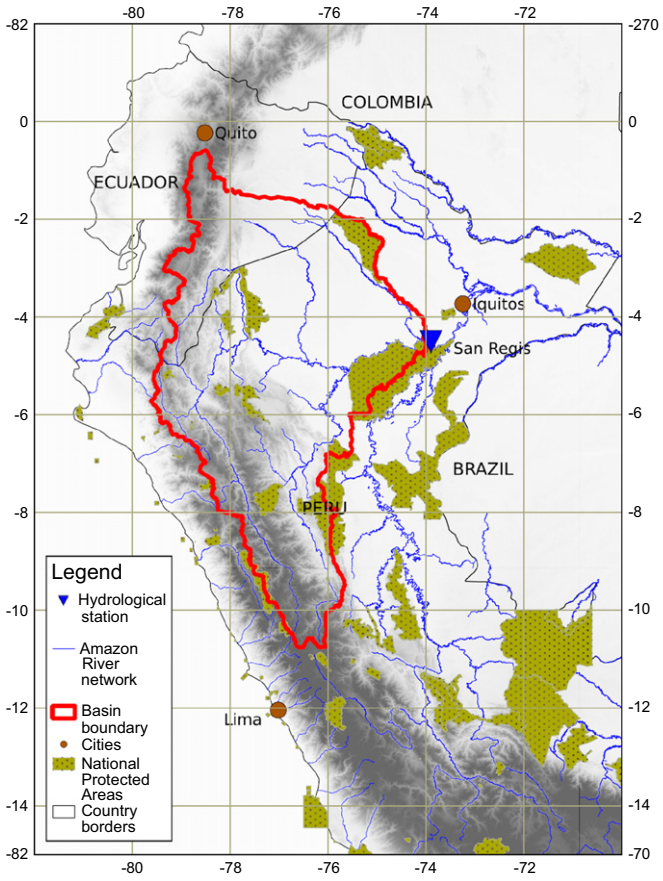

Figure 1. Location map of the Peruvian Amazon basin. The downstream limit is a hydrological station located in San Regis and within the Pacaya–Samiria National Reserve, approximately 130 km Southwest of Iquitos, Peru.

a statistically significant increase since the 1990s, which may be explained by wet season (MAM) precipitation increases linked to a positive geo-potential anomaly South of the equator [9, 10]. These climate anomalies are thought to be the primary cause of major flooding events in 1999, 2009 and 2012 in the Peruvian Amazon [2]. Although strong dry periods have occurred in 2005 and 2010 [11–14], these are thought to represent localised lows in an overall long-term increasing trend in precipitation, temperature, and runoff [9]. We investigate whether this increasing trend may continue throughout the 21st century in response to increasing precipitation, which would contrast the climatic drying projected for the lower Amazon.

Locally known as the Marañón, the Peruvian Amazon river originates in the Northern Peruvian and Southern Ecuadorian Andes (figure 1). At San Regis, a hydrological station 130 km upstream of the city of Iquitos, the tributary drainage area of the river amounts to 360 000 km^2 and the river records an average discharge of 17 500 $m^3 s^{-1}$ (1984–2014). The basin is subject to multiple synoptic meteorological drivers such as the Intertropical Convergence Zone, South American Monsoon System, and El Nino Southern Oscillation (ENSO). Combined with large gradients in altitude, aspect and orography, this generates complex local microclimates [15–17]. More than 75% of the area is covered by mountain and lowland rainforests, while the higher regions are dominated by drier grass- and shrublands.

A large part of the catchment is covered by the Ucamara depression, which comprises the lowland region between the Marañon and the Ucayali rivers. It consists of an intricate network of white and black water rivers with an extreme amplitude in seasonal water level, ranging between 5 and 8 m [18, 19]. In this region, single-pulse flooding regulates species movement and reproduction processes by governing the availability and distribution of their habitats such as temporary lakes, sand beaches and seasonal flood forests (vàrzeas) in the floodplain [20, 21]. This annual flooding cycle not only strongly influences local eco-hydrology but also the economic processes of the people inhabiting the floodplain [21].

In section 2, we describe a methodology for assessing the potential impact of future climate change on the hydrological regime of the Peruvian Amazon river. We use the ensemble model output from the Coupled-Model Intercomparison Project Phase 5 (CMIP5), as forcings to a physics-based distributed hydrological model to produce historical and future projections of flow in the Peruvian Amazon river. The projections of flow are bias-corrected using daily observation of

flows and an extreme value analysis is conducted to derive cumulative probability distributions of the annual mean and extremes (low and high flows, section 3). The results are discussed (section 4) in the context of the broader literature on climate change in Western Amazonia, in particular, the potential implications for the local hydro-ecology of the floodplain.

2. Methods and data

2.1. Land surface hydrological modelling

The Joint-UK Land Environment Simulator (JULES, [22]) is the research version of the physics-based land surface scheme used to provide the boundary conditions in weather and climate models of the UK Meteorological Office. In an offline simulation, it takes input of meteorological time series of temperature, pressure, humidity, radiation, precipitation, and wind speed, and solves full energy and water balance equations for estimating aggregate surface fluxes such as latent heat and runoff. The model has been previously implemented over the Peruvian Amazon [23, 24]. A summary and updates to the model are described here.

JULES is paramaterised over the Peruvian Amazon basin using 2040 grid cells of 0.125° by 0.125° (14 km × 14 km). In the model evaluation, the model is forced using bias-corrected and spatially disaggregated reanalysis of surface temperature, pressure, specific humidity, radiation, wind speed data from Princeton Hydrology [25] and precipitation data from TRMM Multi-satellite Precipitation Analysis version 7 [26], which are corrected at the daily scale using rain gauge data from 179 stations from the Servicio Nacional de Meteorología e Hidrología, Peru (SENAMHI). To improve estimation of surface and subsurface runoff, the simulations are performed with a sub-grid representation of the soil moisture heterogeneity using the probability distributed model. The 'b' parameter that controls the shape of the distribution of the sub-grid storage capacity is modelled as a function of slope at each model grid.

Surface and subsurface runoff from each model grid is then routed to the outlet in parallel using delay functions and assuming constant celerities along the river flow and subsurface flow network derived using digital terrain map. At the outlet, an overbank flow threshold is imposed on the calculated total runoff. Flow above this threshold is rerouted in a linear store representing additional attenuation within the floodplain. A constant sink term is added to this overflow to represent loss due to ponded water evaporation. The final attenuated flows are compared against daily records of streamflow at San Regis, available through HYBAM (geodynamical, HYdrological and Biogeochemical control of erosion alteration and material transport in the AMazon Basin) from SENAMHI during the period between 1984–2015.

2.2. Climate change impact modelling and model-bias correction

In the climate change simulation, Global Climate Model (GCM) projections of precipitation, temperature, pressure, specific humidity, wind speed, and radiation are obtained through the British Atmospheric Data Centre data archive. Simulation results of 18 models from the RCP 4.5 and 8.5 scenarios of the ensemble are used to drive JULES to produce 20th and 21st century projections of daily flows. The model output over the historical (1976–2005) and future projection (2006–2035, 2036–2065, 2066–2095) periods are bias-corrected using the equidistant quantile mapping [27] adapted to river flows, using a coincident 22 yr (1984–2005) historical daily observations of river flows. In the quantile mapping, relative bias factor values are calculated at every 0.001 quantile between the cumulative distribution function (CDF) of the simulated flows for the historical period relative to the CDF of the observed flows. These quantile-based change factors are then applied to the CDF of the projected flows to obtain the bias-corrected future projections for the basin. The bias correction is performed as a two-step correction—the first corrects for hydrological event (annual) volumes and the second corrects for the distribution of daily flows. This is described step-by-step as follows:

(i) The separation between the wet and dry seasons for each year is identified. Here we use the first point after the flood peak when the total flow reduces to baseflow contributions. The baseflow is determined from the observation time series using a low pass digital filter [28]. The flows between this point in a given year and that in the subsequent year constitutes one annual hydrological 'event' OBS. $Q_{i,t}$ for $i = 1, 2, \ldots, n$, where n = total number of events and $t = 1, 2, ..., T$, where T = total number of days in event i.

(ii) The volume of flows during each event is calculated as the area under the hydrograph:

$$\text{OBS.}V_i = \sum_{t=1}^{T} \text{OBS.}Q_{i,t}\,\mathrm{d}t.$$

(iii) (i)–(ii) are repeated on the daily GCM historical and future projections of flows GCMhist.$Q_{i,t}$ and GCMfut.$Q_{i,t}$ to produce the GCM-based time series of volumes GCMhist.V_i and GCMfut.V_i respectively.

(iv) A quantile-based relative bias correction model is developed based on the distributions of GCMhist.V_i and OBS. V_i, i.e. the bias factor BF at each quantile q is calculated as follows where F_X is the cumulative probability function:

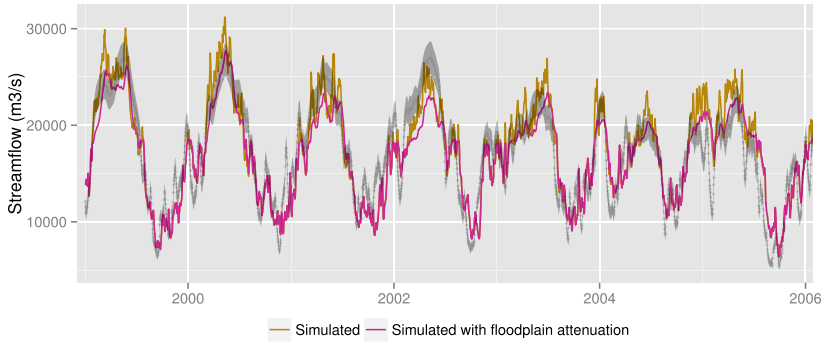

Figure 2. The observed and simulated historical streamflow at San Regis. The hydrographs of the river are shown for the period 1999–2005. The observed flow is shown in grey with the band representing observation uncertainty. Simulated flow is shown both without and with attenuation through the floodplain store.

$$\mathrm{BE_q} = \frac{F_X(\mathrm{OBS}.V)_\mathrm{q}}{F_X(\mathrm{GCMhist}.V)_\mathrm{q}}$$

and the corrections are applied to GCMfut.V to produce GCMfut .V_{BC}.

(v) To redistribute the volume correction at the daily scale, the difference between the uncorrected and corrected event volumes is computed for each event i. This difference is reassigned proportionally by the day's relative volume to the event volume:

$$\mathrm{GCMfut}.Q_{\mathrm{BC},i,t} = \mathrm{GCMfut}.Q_{i,t} + \frac{\mathrm{GCMfut}.Q_{i,t}}{\sum_{t=1}^{T}\mathrm{GCMfut}.Q_{i,t}} \times (\mathrm{GCMfut}.V_{\mathrm{BC},i} - \mathrm{GCMfut}.V_i).$$

(vi) A similar quantile based relative bias correction is performed to adjust the CDFs of discharges.

2.3. Extreme value analysis

The above procedure is repeated for each model within the CMIP5 ensemble, and each of the RCP 4.5 and 8.5 scenarios, to produce a time series of historical and future projections for each case. From this, the annual values of the minimum (AMIN), mean (AMEAN) and maximum (AMAX) flows are calculated. For each 30 yr historical and future projection periods, each RCP scenario, and each GCM, a generalised extreme value distribution (GEVD) is fitted on the annual time series using the L-moment method to produce the return periods of extreme events.

For details of the L-moment method, the reader is referred to [29, 30], but a summary is included here for completeness. The GEVD has CDF:

$$F(x;\,\mu,\,\sigma,\,\xi)\exp\left\{-\left[1+\xi\left(\frac{x-\mu}{\sigma}\right)\right]^{-1/\xi}\right\} \quad (1)$$

for $1+\xi(x-\mu)/\sigma > 0$, where $\mu \in \mathbb{R}$ is the location parameter, $\sigma > 0$ the scale parameter and $\xi \in \mathbb{R}$ the shape parameter. The shape parameter defines whether the distributions belong to the Gumbel (exponential tail, $\xi = 0$), Fréchet (polynomial 'fat' tail, $\xi > 0$) or reverse Weibull (upper bound, $\xi < 0$) family. These parameters are estimated as functions of the L-moments of the sample (i.e. values of the time series of AMIN, AMEAN, or AMAX), in the assumption that these are equal to the L-moments of the GEVD. L-moments are analogous to conventional moments (mean, variance, skew, and kurtosis) but calculated based on a linear combination of the order statistics of the sample.

The L-moment method provides computationally efficient, robust estimates in cases of small samples [29]. There are uncertainties associated with the parameter estimation. However, statistical uncertainties have been argued to be minor relative to the remaining uncertainty in GCM [31], and we assume that this is the case for the Peruvian Amazon. Furthermore, our results (figure 4) show that the ensemble approach is able to average out the individual errors and reproduce the distribution of historical extremes. Future work can focus on formal characterisation of the different sources of errors, incorporating non-stationarity into the bias correction, and/or doing a fully fledged physics-based and distributed downscaling of the climate using a regional climate model.

3. Results

The flow regime of the Peruvian Amazon river is characterised by small daily variations superimposed on a strong seasonal component (figure 2). We simulated the rainfall–runoff relation of the river during the historical period 1999–2005, and obtained a Nash–Sutcliffe efficiency score of 0.77 and 0.85 at the respective daily and monthly time-scales. The upper percentiles (90th, 95th, and 99th) of the daily streamflows are modelled within 5% error, indicating the model's ability to simulate daily extremes (table 1). The model also captures floodplain attenuation and times-to-peak, both of which are critical hydrological

Table 1. The historical simulation of the hydrological extremes (daily) at San Regis compared to observations (1999–2005).

Percentile	1	5	10	50	90	95	99
Observed	6663	8441	9996	17 123	23 689	24 984	26 704
Modelled	7978	9852	10 823	18 055	22 737	24 665	26 358
Relative error (%)	19.76	16.71	8.28	5.44	−4.02	−1.27	−1.30

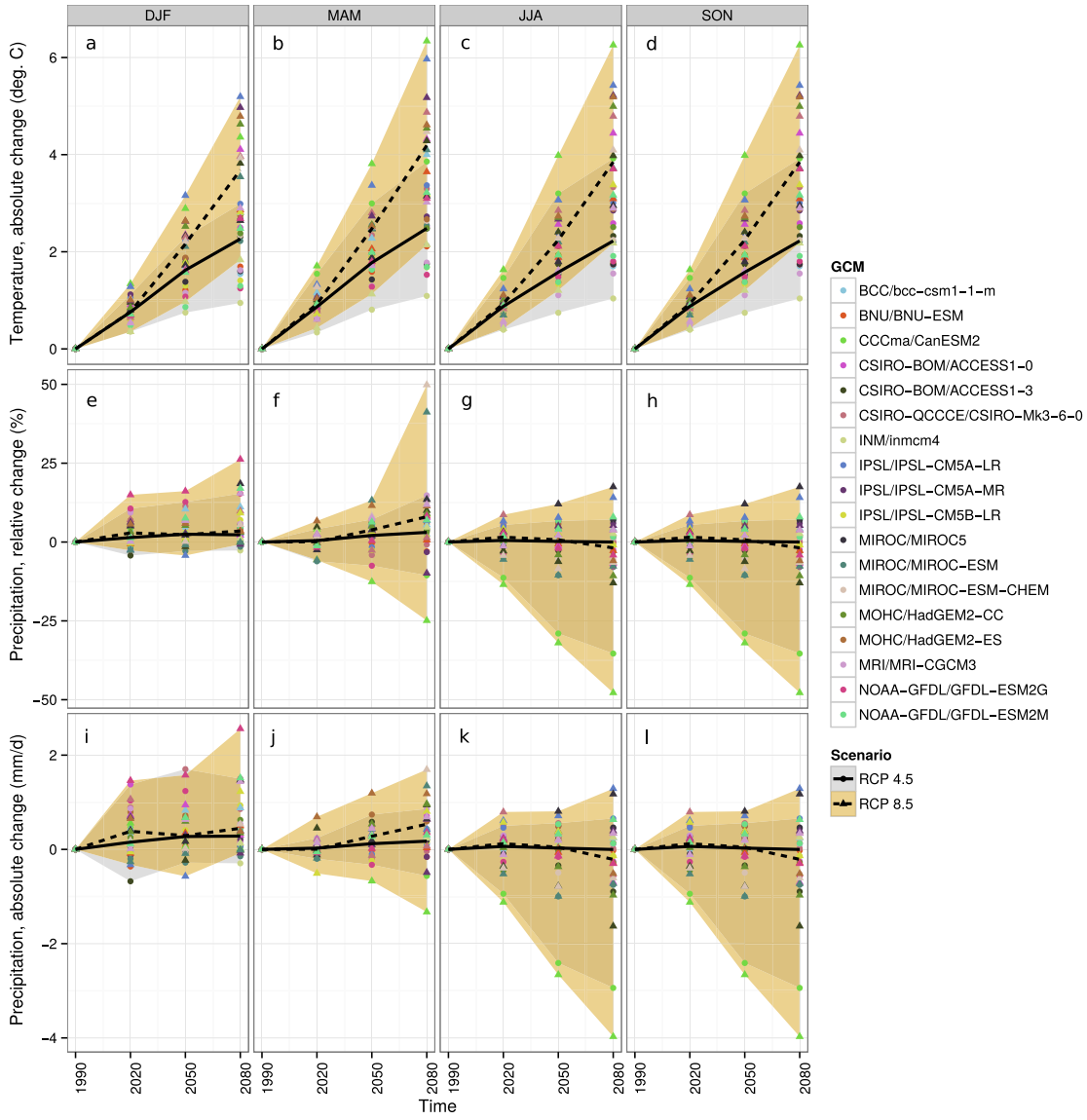

Figure 3. 30 yr mean seasonal anomalies in the Peruvian Amazon with inter-GCM variability. For temperature (a)–(d), the anomaly is an absolute value with zero as the baseline, and values larger (smaller) than zero indicate an increase (decrease). For precipitation (e)–(h), the anomaly is a relative value with zero as the baseline, and values larger (smaller) than one indicate an increase (decrease); additionally absolute magnitudes of change in mm d^{-1} are also presented (i)–(l). Each dot is the areal average of a model projection for the entire Peruvian Amazon basin.

functions to represent prior to higher temporal aggregation for the extreme value analysis.

The CMIP5 projections of the climate over the Peruvian Amazon are presented in terms of the change in annual basin average in 30 yr periods centred on 2020, 2050, and 2080, relative to the 30 yr historical reference period centred on 1990, for two representative concentration pathways, RCP 4.5 and RCP 8.5 (figure 3). During the wet season (MAM; figures 3(b), (f) and (j)), surface air temperatures are projected to increase with an ensemble mean of +4.1 °C and +2.2 °C in the RCP 8.5 and RCP 4.5 scenarios respectively towards the end of the 21st century. RCP 8.5 scenario also shows a stronger mean signal for precipitation increase during MAM, with an 8% increase compared to 3% under RCP 4.5. Meanwhile the dry season (SON; figures 3(d), (h) and (l)) precipitation indicates an initially increasing and

subsequently decreasing mean signal. Under the RCP 8.5 scenario, the net change becomes negative (−3%) by the end of the analysis period.

We analyse the propagation of this strengthening of the precipitation seasonality to the river flow, and find an overall increase of the river flow due to a dominating wet season under the RCP 8.5 scenario (figure 4). Based on the ensemble means, projections for the future indicate an upward shift in the values of AMIN, AMEAN and AMAX flows over the range of return periods. On the other hand, under the RCP 4.5 scenario, increases in the extremes are only observed with AMAX (figure 4(e)). In fact, the only pronounced hydrological impact of climate change is the increase in AMAX, which proxies for the wet season peak floods. RCP 8.5 projects a continuous increase in extreme flood magnitudes towards the final 30 yr period (figure 4(f)). The 100 yr return flow is expected to increase by 12% (ensemble range between −11% and +35%) relative to the historical reference period. In contrast, AMAX increases initially under RCP 4.5, exceeding those of RCP 8.5 mid-century, but decreases after 2065 with a net increase of 7.5% (ensemble range between −17% and 33%) for the 100 yr return flow relative to the historical period. Such transient behaviour may be attributed to transient climatic changes, as shown by the increase in dry season precipitation during the beginning of the 21st century and a subsequent decrease. Similarly during the wet season (DJF), precipitation increases at a higher rate in the earlier part of the century.

Large variations within the ensemble are evident, both in the GCM climate projections themselves and the consequent impact on the hydrological extremes. While diverging responses driven by different climate models is a fundamental property of ensemble modelling, the strongly diverging signal of a few GCMs either heavily distorts or dilutes the mean change signal of the ensemble. A case in point is the GCM Can-ESM2 which projects a much drier and warmer climate compared to the remaining GCMs in the ensemble (figures 3(b)–(d)). The anomaly could be caused by many factors including the coarse GCM resolution effectively lowering the topographic barrier presented by the Andean ranges and poor representation of tropical hydro-meteorological processes within the climate models. Nevertheless, the majority of the GCMs in the ensemble indicates a hydrological change towards wetter conditions. For instance, 10 (13) out of 18 models project an increase in the 100 yr return value for AMIN (AMAX) respectively under the RCP 8.5 scenario. Similarly, 11 out of 18 models project an increase in the 100 yr return value for AMAX under the RCP 4.5 scenario.

These results should be interpreted in the context of the model assumptions and limitations. Firstly, we assume stationarity over the historical period that is used to generate the baseline statistics on which the bias correction model is applied. However, earlier research [32] has shown that climate in the region is oscillating over time spans of few decades; for the Ecuadorian Andes, for instance, our study's historical period 1984–2005 spans approximately one climate oscillation cycle, and therefore, any trends over that period in our study area may be expected to be part of the longer term climate variations. Secondly, the probability distributions (return periods) were produced using annual flow statistics over 30 yr GCM periods, which may result in some uncertainty around the fitted distributions. However, as discussed in section 2.3, we assume this uncertainty to be relatively small compared to climate model uncertainty. A further limitation may come from the land surface model, which has no representations of local storages [23] and is coupled offline to hydrological routing that limits the potential of water returning to the land surface and atmosphere; hence ET and runoff may be systematically under- and overestimated and impact the simulation of dry and wet season extremes. To partially address this, a lumped linear store model is introduced at the basin scale with a sink term to replicate the floodplain storage functions and induce additional ET loss from a high water table during the wet season.

4. Discussion and conclusion

Our study shows that the changes in extremes projected in the Peruvian Amazon to be related to a a strengthening seasonality of precipitation in the region. Several authors have suggested potential explanations for wet season precipitation increase in the late 21st century: e.g. enhanced convective activities from surface warming [33]; intensifying ENSO and Atlantic Multidecadal Oscillation as there is evidence of teleconnectivity between the sea surface temperatures in the Pacific and Atlantic and precipitation in the basin [34]; intensifying monsoon systems [6, 35].

Several studies have also looked into the hydrological impact of the change in climate, but focusing mostly on the impact on soil moisture and its links to rainforest resilience [3–6]. The consequence of forest dieback can be adverse, as the conversion of the system from a carbon reserve to a carbon source may positively feedback to climate [36]. This has been predicted in Southeastern Amazonia as a result of water stress during extended periods of drought that drives the rainforests towards their 'tipping point', beyond which they can no longer recover [4, 37, 38]. In the Western Amazon however, the CMIP5 ensemble shows more agreement on an increase in precipitation. This makes it imperative to quantify change river flow regimes, in particular because of the potentially strong impact of changes in peak flows. Our results agree with the predictions under the previous AR4 projections, which also show increases to the 90th percentile monthly flow further downstream in west Brazil [A1B scenario, 39]; similarly 30 yr mean increases exceeding

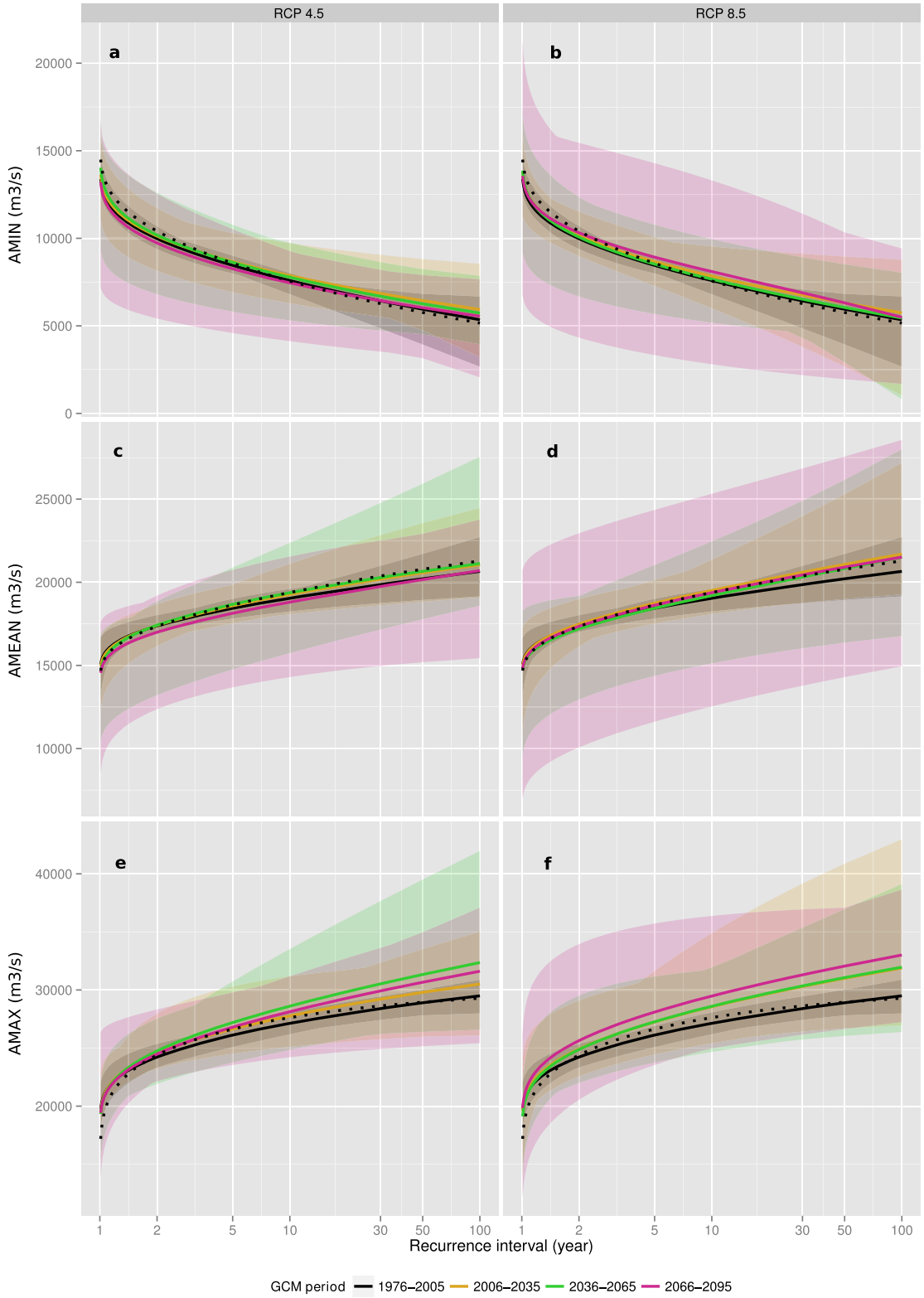

Figure 4. Ensemble projections of future hydrological extremes. The projections based on RCP 4.5 and RCP 8.5 scenarios of climate change are presented in terms of the change in the return periods of the annual minimum, mean, and maximum flows from the historical reference period (black line) to future projection periods. The probability of an event of a certain magnitude can be computed from the inverse of the corresponding return period. The black dots represent the return periods values calculated using the observation time series (1984–2005).

50% were reported in Huallaga river, a tributary of the Peruvian Amazon and Ucayali river to the South [8], as well as a prolonging of the flood inundation of up to 3 months in the region [40].

The hydrological change projected in the Peruvian Amazon will simultaneously impact multiple river-supported processes. In-stream, three distinct types of well-documented hydro-ecological processes can be

identified. Firstly, reptiles and fish rely on algae, whose photosynthetic activities hinge upon nitrogen and phosphorus supplied during annual floods [41]. More extreme floods will therefore increase the river productivity. Secondly, changes to the river regulation will also affect adult catfish migration upriver for spawning and larvae transport downriver, which not only depend on the longitudinal and lateral river connectivity but also on the interplay of hydrological flow events [42]. Modelling approaches have identified increased frequency and flood duration to increase larvae release; moreover, variations in water conductivity between dry to wet season are thought to be a chemical signal that sets migratory routes [43]. Thirdly, native freshwater turtles such as charapa (*Podocnemis Expansa*) and taricaya (*Podocnemis unifilis*), rely on the sand banks deposited after flooding as their breeding grounds. Optimal sediment structure ensures nest structure stability and optimal thermal conductivity, both of which are crucial factors for the viability and the sex proportion of the eggs [44]. A changing river flooding regime can therefore be disruptive to the reproduction processes of these in-stream species, which are also income sources for the floodplain communities [45].

Furthermore, increasing floods is likely to impact the region's swamp forest ecology. Aguaje palm swamps (*Mauritia flexuosa*) are a prominent feature and important source of below-ground carbon pools in the floodplain, along with the seasonal flooded forests (varzeás, [46]). Whether the palms will adapt and thrive, or asphyxiate as a result of prolonged flooding, is a relevant question at multiple scales. At the global scale, the freshwater swamps play an important role in carbon cycling, whereas locally, the palms provide commercially valuable fruits and raw material for furniture. Any changes in their ecology will necessarily have local socio-economic aspects, as indigenous groups inhabiting the floodplains have over time developed a local economy closely linked to the inundation pattern of the river. Increasing extremes will also create a greater flood risk to the riverine settlements who cultivate along the river banks and rely on a sustained volume of flows for agriculture and water quality [2].

Nonetheless, the impact of climate change should be seen in a wider context of human-induced hydrological change, including also land-use change and dam construction, whereby 54% of the total number of dams in the next 20 yr in the Peru, Ecuador, Colombia, and Bolivia are projected to be located in this basin [47]. Given the potential ecological and socio-economic impacts, a better understanding the interplay between these different drivers on the hydrology of this region is highly timely.

Acknowledgments

ZZ and WB acknowledge funding from UK Natural Environment Research Council NE-K010239-1 (Mountain-EVO) and NE/I004017/1 (VO-ESPA).

References

[1] Pokhrel Y N, Fan Y and Miguez-Macho G 2014 *Environ. Res. Lett.* **9** 084004
[2] Espinoza J, Guimberteau M, Guyot J L, Lavado W J R and Santini W 2014 El perù frente al cambio climático—resultados de investigaciones franco-peruanas *Eventos Hidrológicos Extremos en la Cuenca Amazonica Peruana: Presente y Futuro* ed A Gr'egoire (Lima, Peru: IRD) pp 47–58 ch 3 (www.peru.ird.fr/content/download/95497/724661/version/9/file/EL+PERU+FRENTE+AL+CAMBIO+CLIMATICO.pdf)
[3] Malhi Y, Roberts J T, Betts R A, Killeen T J, Li W H and Nobre C A 2008 *Science* **319** 169–72
[4] Nepstad D C, Stickler C M, Filho B S and Merry F 2008 *Phil. Trans. R. Soc.* B **363** 1737–46
[5] Brando P M, Goetz S J, Baccini A, Nepstad D C, Beck P S A and Christman M C 2010 *Proc. Natl Acad. Sci.* **107** 14685–90
[6] Boisier J P, Ciais P, Ducharne A and Guimberteau M 2015 *Nat. Clim. Change* **5** 656–60
[7] Espinoza J, Ronchail J, Frappart F, Lavado W, Santini W and Guyot J 2013 *J. Hydrometeorology* **14** 1000–8
[8] Lavado-Casimiro W S, Labat D, Guyot J L and Ardoin-Bardin S 2011 *Hydrol. Process.* **25** 3721–34
[9] Gloor M, Brienen R J W, Galbraith D, Feldpausch T R, Schngart J, Guyot J L, Espinoza J C, Lloyd J and Phillips O L 2013 *Geophys. Res. Lett.* **40** 1729–33
[10] Villar J C E, Guyot J L, Ronchail J, Cochonneau G, Filizola N, Fraizy P, Labat D, de Oliveira E, Ordonez J J and Vauchel P 2009 *J. Hydrol.* **375** 297–311
[11] Marengo J A, Nobre C A, Tomasella J, Oyama M D, De Oliveira G S, De Oliveira R, Camargo H, Alves L M and Brown I F 2008 *J. Clim.* **21** 495–516
[12] Marengo J A, Tomasella J, Alves L M, Soares W R and Rodriguez D A 2011 *Geophys. Res. Lett.* **38** L12703
[13] Lewis S L, Brando P M, Phillips O L, van der Heijden G M F and Nepstad D 2011 *Science* **331** 554–554
[14] Tomasella J, Borma L S, Marengo J A, Rodriguez D A, Cuartas L A A, Nobre C and Prado M C R 2011 *Hydrol. Process.* **25** 1228–42
[15] Buytaert W, Célleri R, Willems P, De Bièvre B and Wyseure G 2006 *J. Hydrol.* **329** 413–21
[16] Garreaud R D, Vuille M, Compagnucci R and Marengo J 2009 *Palaeogeogr. Palaeoclimatol. Palaeoecol.* **281** 180–95
[17] Espinoza-Villar J, Ronchail J, Guyot J L, Cochonneau G, Naziano F, Lavado W, De Oliveira E, Pombosa R and Vauchel P 2009 *Int. J. Climatol.* **29** 1574–94
[18] Dumont J F 1991 *Géodynamique* **6** 9–20 (www.documentation.ird.fr/hor/fdi:41472)
[19] Räsänen M, Neller R, Salo J and Jungner H 1992 *Geol. Mag.* **129** 293–306
[20] Junk W J, Bayley P B and Sparks R E 1989 *Canadian Special Publication of Fisheries and Aquatic Sciences* **106** 110–127
[21] Kvist L P, Gram S, Cácares C A and Ore B I 2001 *Forest Ecology Manage.* **150** 175–86
[22] Best M J *et al* 2011 *Geoscientific Model Development* **4** 677–99
[23] Zulkafli Z, Buytaert W, Onof C, Lavado W and Guyot J L 2013 *Hydrol. Earth Syst. Sci.* **17** 1113–32
[24] Zulkafli Z, Buytaert W, Onof C, Manz B, Tarnavsky E, Lavado W and Guyot J L 2014 *J. Hydrometeorology* **15** 581–92
[25] Sheffield J, Goteti G and Wood E F 2006 *J. Clim.* **19** 3088–111
[26] Huffman G J and Bolvin D T 2014 NASA, Greenbelt, USA 1–40 (ftp://precip.gsfc.nasa.gov/pub/trmmdocs/3B42_3B43_doc.pdf)
[27] Li H, Sheffield J and Wood E F 2010 *J. Geophys. Res. Atmos.* **115** D10101
[28] Lyne V and Hollick M 1979 *Institution of Engineers Australia National Conference Publication* **79/10** 89–93
[29] Hosking J R M 1990 *J. R. Stat. Soc.* B **52** 105–24 (www.jstor.org/stable/2345653)
[30] Hosking J R M 1992 *Am. Stat.* **46** 186–9
[31] Wehner M 2010 *Extremes* **13** 205–17
[32] Mora D and Willems P 2012 *Theor. Appl. Climatol.* **108** 267–82
[33] Liu C and Allan R P 2013 *Environ. Res. Lett.* **8** 034002

[34] Duffy P B, Brando P, Asner G P and Field C B 2015 *Proc. Natl Acad. Sci. USA* **112** 13172–7
[35] Urrutia R and Vuille M 2009 *J. Geophys. Res. Atmos.* **114** D02108
[36] Phillips O L *et al* 2009 *Science* **323** 1344–7
[37] Hilker T, Lyapustin A I, Tucker C J, Hall F G, Myneni R B, Wang Y, Bi J, Mendes de Moura Y and Sellers P J 2014 *Proc. Natl Acad. Sci. USA* **111** 16041–6
[38] Malhi Y, Aragão L E, Galbraith D, Huntingford C, Fisher R, Zelazowski P, Sitch S, McSweeney C and Meir P 2009 *Proc. Natl. Acad. Sci. USA* **106** 20610–5
[39] Guimberteau M, Ronchail J, Espinoza J, Lengaigne M, Sultan B, Polcher J, Drapeau G, Guyot J L, Ducharne A and Ciais P 2013 *Environ. Res. Lett.* **8** 014035
[40] Langerwisch F, Rost S, Gerten D, Poulter B, Rammig A and Cramer W 2013 *Hydrol. Earth Syst. Sci.* **17** 2247–62
[41] Melack J M and Forsberg B R 2001 Biogeochemistry of Amazon floodplain lakes and associated wetlands *The Biogeochemistry of the Amazon Basin* ed M E McClain *et al* (Oxford: Oxford University Press) pp 235–276 ch 14
[42] Cañas C and Pine W 2011 *River Res. Appl.* **27** 602–11
[43] Cañas C M and Waylen P R 2012 *Hydrol. Process.* **26** 996–1007
[44] de Souza R R and Vogt R C 1994 *J. Herpetology* 453–64
[45] Gockel K and Gray L 2009 *Ecol. Soc.* **14** 11 (www.ecologyandsociety.org/vol14/iss2/art11)
[46] Draper F C, Roucoux K H, Lawson I T, Mitchard E T, Coronado E N H, Lähteenoja O, Montenegro L T, Sandoval E V, Zaráte R and Baker T R 2014 *Environ. Res. Lett.* **9** 124017
[47] Finer M and Jenkins C N 2012 *Plos One* **7** e35126